ISSN 0016-7029, Geochemistry International, 2023, Vol. 61, No. 7, pp. 669–686. © Pleiades Publishing, Ltd., 2023.
Russian Text © The Author(s), 2023, published in Geokhimiya, 2023, Vol. 68, No. 7, pp. 651–668.

Feldspar Megacrysts as a Source of Information on Crustal Contamination of Basaltic Melt

E. I. Demonterova[a], *, A. V. Ivanov[a], **, S. V. Palessky[b], V. F. Posokhov[c], N. S. Karmanov[b], and L. A. Pel'gunova[d]

[a] *Institute of the Earth's Crust, Siberian Branch, Russian Academy of Sciences, Irkutsk, 664033 Russia*
[b] *Sobolev Institute of Geology and Mineralogy, Siberian Branch, Russian Academy of Sciences, Novosibirsk, 630090 Russia*
[c] *Dobretsov Geological Institute, Siberian Branch, Russian Academy of Sciences, Ulan-Ude, 670047 Russia*
[d] *Severtsov Institute of Problems of Ecology and Evolution, Russian Academy of Sciences, Moscow, 117198 Russiat*
**e-mail: dem@crust.irk.ru*
***e-mail: aivanov@crust.irk.ru*

Received June 19, 2022; revised July 19, 2022; accepted February 3, 2023

Abstract—The paper discusses data on the elemental composition and $^{87}Sr/^{86}Sr$, and $\delta^{18}O$ isotopic ratios of feldspar megacrysts collected from lava flows, tuffs, and cinders of three volcanic fields in the Baikal rift system: Iya–Uda, Vitim, and Khamar-Daban, which are located within the early Precambrian, Riphean, and Paleozoic crustal blocks, respectively. Megacrysts are hosted in trachybasalts in the Iya–Uda and Khamar-Daban fields and in basanites in the Vitim field. Megacrysts belong to the following three compositional groups of minerals: (i) plagioclase in lavas of the Iya–Uda field, (ii) anorthoclase in lava flows, tuffs, and cinders of the Khamar-Daban and Vitim fields, and (iii) sanidine in the Vitim field. Elemental and isotope data suggest that megacrysts crystallized in volcanic chambers at different depth levels: anorthoclase crystallized from the most primitive magma with mantle-derived isotopic signatures at subcrustal depth levels, plagioclases were produced in deep crustal chambers during the interaction between mantle-derived magma and crustal rocks, and sanidine was captured from the upper crustal rocks.

Keywords: feldspars, megacrysts, basalts, Baikal rift
DOI: 10.1134/S0016702923070029

INTRODUCTION

Magmatic rocks are produced in various geological settings most commonly contain feldspar megacrysts (the term *megacryst* therewith does not a priori imply any genetic interpretation and refers solely to the size of the crystals). Interpretations of the circumstances under which megacrysts are formed are disputable, regardless of whether they are phenocrysts (i.e., crystallized from the same magma that entrained them), xenocrysts (i.e., are foreign to the magma), or antecrysts (i.e., crystallized by another magma than that entrained them but were related to this magma within a single continuous magmatic process). Cenozoic volcanic rocks in the Baikal rift system and adjacent territories in Mongolia are no exception: feldspar megacrysts were found in all of the basalt volcanic fields. However, feldspar megacrysts are not ubiquitous but occur only in some of the lava flows, tuffs, and cinders of the volcanic edifices, and various models were put forth to explain their genesis (Volyanyuk et al., 1978; Rasskazov, 1985; Ashchepkov, 1991; Litasov and Mal'kovets, 1998; Ashchepkov et al., 2011; Perepelov et al., 2020).

The crystallization parameters of megacrysts and their relationships with the melts entraining them still remain a matter of discussion. The two major hypotheses are as follows. Some researchers believe that feldspar inclusions crystallized from the entraining magma (Guo et al., 1992; Lundstrom et al., 2005; Higgins, Chandrasekharam, 2007), whereas others argue that feldspar inclusions are xenogenic and are not genetically related to the entraining melts (Perini, 2000; Akinin et al., 2005; Ashchepkov et al., 2011). It was not until recently that the concept of antecrysts was formulated: they are understood as crystals that crystallized in a deep magma chamber not from the magma portion that entrained them to the surface, but such a crystal is therewith genetically related to the magmatic system as a whole (Hildreth, 2001). Our publication presents the elemental and isotope ($^{87}Sr/^{86}Sr$ and $\delta^{18}O$) compositions of feldspar megacrysts in Late Cenozoic lava flows, tuffs, and cinders of the Iya–Uda, Vitim, and Khamar-Daban volcanic fields of the Baikal rift (Fig. 1). We used our data on these megacrysts to justify a generalized model for the crystallization of megacrysts in volcanic chambers both

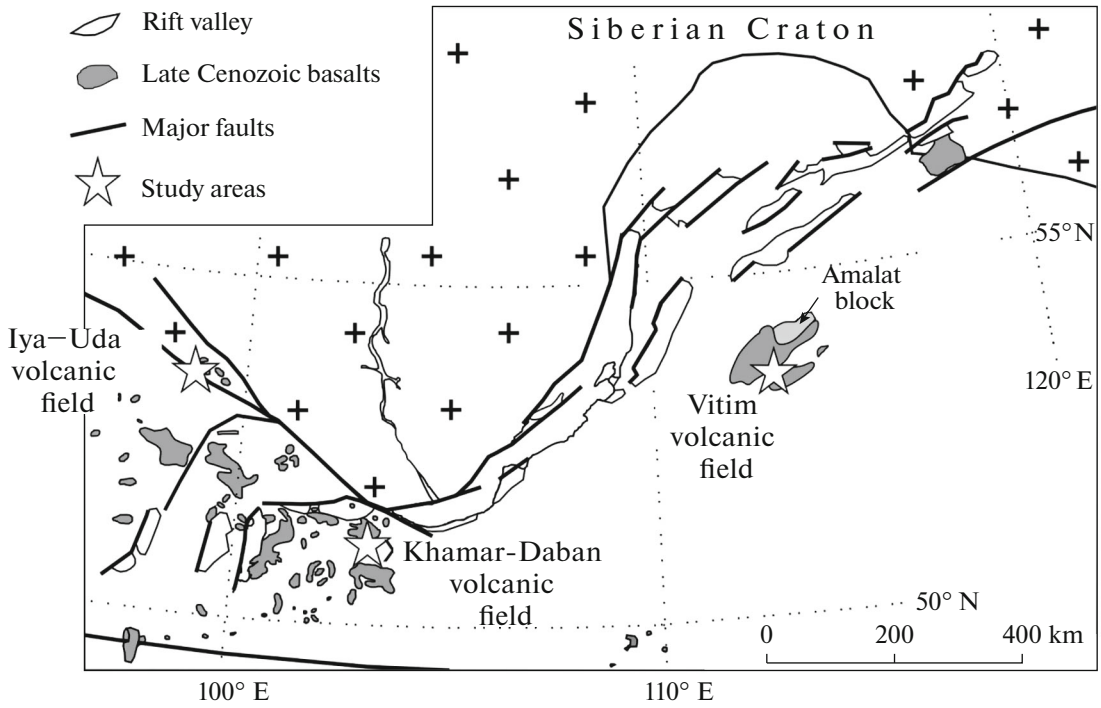

Fig. 1. Schematic location map of the volcanic fields relative to the Baikal rift system. Stars mark our study areas.

from primitive magma and at its interaction with crustal rocks of various chemical and isotope composition.

MATERIALS

Khamar-Daban Volcanic Field

The rocks of the Khamar-Daban volcanic field make up the mountaintops of the Khamar-Daban Range in the southern part of the Baikal rift, near the southern tip of Lake Baikal (Fig. 1). The volcanoes and lava flows occur among the early Paleozoic magmatic and metamorphic rocks of the Khamar-Daban terrane (Belichenko et al., 1994). Megacrysts of K–Na feldspars are widespread in some of the lava flows, tuffs, and cinders dated at 16.9–12.6 Ma and occurring in the upper reaches of the Tumusun and Usun rivers (Ivanov et al., 2015). Feldspar megacrysts were sampled from several flows and tuffs of the vocano Tumusun. The summit part of this volcano consists of a pyroclastic unit crosscut by dikes. The very top of the mount is made up of a neck with abundant lherzolite nodules (Ashchepkov, 1991; Ionov et al., 1995). The total thickness of the lava pile of the volcano Tumusun is about 500 m. Feldspar inclusions were found at various hypsometric levels in the lava edifice. They are transparent crystals with clearly seen cleavage and melted margins. They vary from 0.5 to a few centimeters (Figs. 2a, 2b, 3). The tuff unit in the summit part of this volcano contains inclusions as large as 10 cm. The tuffs are relatively loose, and numerous feldspar megacrysts are thus accumulated at the foot of this unit when the tuff is disintegrated. The rocks hosting of megacrysts correspond to basanite and trachybasalt in composition.

Iya–Uda Volcanic Field

The late Cenozoic volcanic flows in the area between the Iya and Uda rivers rest on the basement of the Siberian Craton in the Biryusa block (Fig. 1), which is made up of Archean–early Proterozoic metamorphic and magmatic rocks, although the block also contains younger (Riphean and early Paleozoic) intrusive rocks (Turkina et al., 2006; Dmitrieva and Nozhkin, 2012; Donskaya et al., 2014). Fragments of the volcanic flows are scattered as remnant blocks over an extensive territory of approximately 2000 km^2 (Burakov and Fedorov, 1954). Feldspar megacrysts were collected from the bottom portion of the lava edifice between the Khadoma and Khoropka rivers (both are right-hand tributaries of the Uda River), which was dated at 4.3 Ma (Demonterova et al., 2017). Megacrysts are as large as 3 cm (Figs. 2c, 2d). The rocks hosting of feldspar megacrysts are trachyandesite in composition.

Vitim Volcanic Field

The Vitim volcanic field occurs away from the axial part of the Baikal rift, east of Lake Baikal. The Vitim field is constrained within the Riphean Amalat block surrounded with early Paleozoic rocks of the Ikat ter-

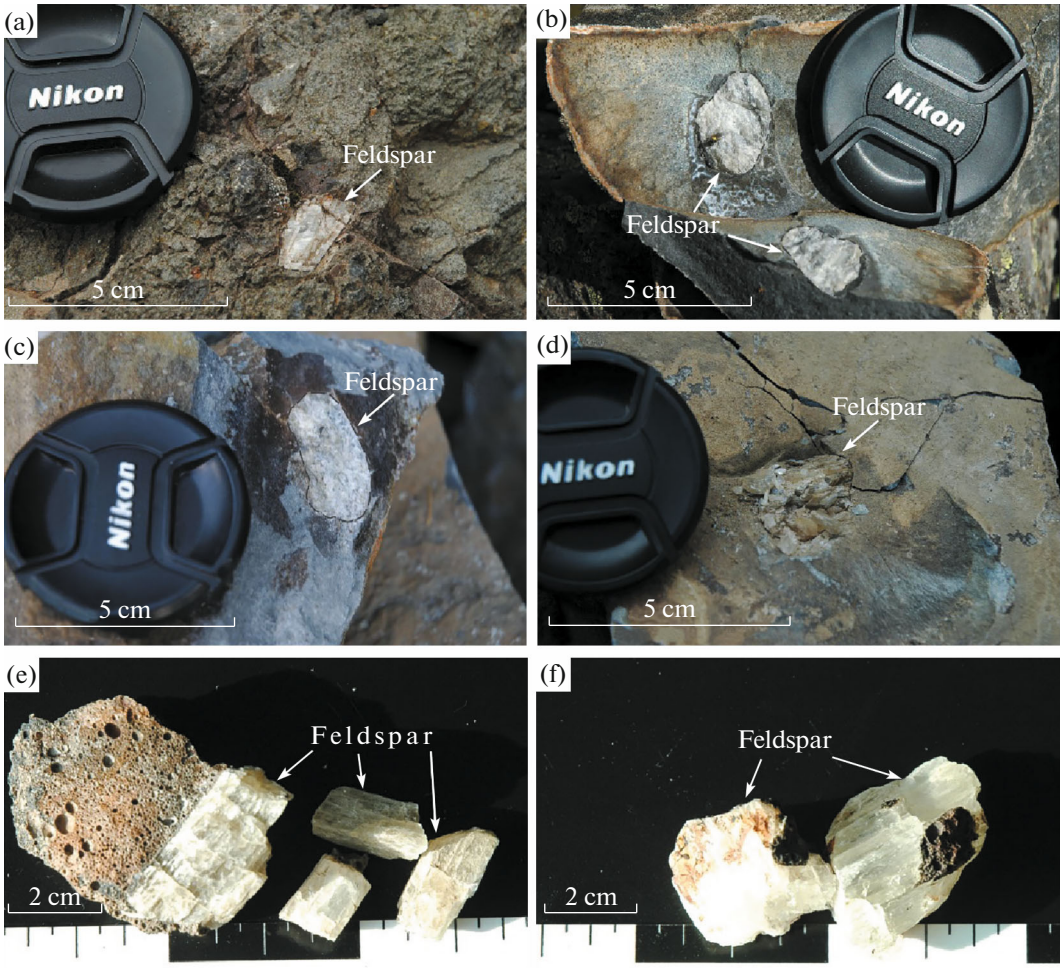

Fig. 2. Feldspar megacrysts in lavas of (a, b) the volcano Tumusun of the Khamar-Daban and (c, d) Iya–Uda volcanic fields, and (e, f) cinders of the volcano Kandidushka, Vitim volcanic field.

rane (Belichenko et al., 2006). Feldspar inclusions were found in the cinders of Quaternary the volcano Kandidushka (Figs. 2e, 2f), which is one of twenty volcano cones of the Vitim field (Kiselev et al., 1979). The volcano has an ejecta rim wall of ~500 m in diameter, which is cut by a road-rubble quarry. The cinder cone raises above a related lava flow, and its rocks were dated at 1.5 Ma (K–Ar) (Ashchepkov et al., 2003). Both the cinder and the lava flow have basanite composition.

ANALYTICAL TECHNIQUES

Prior to studying the elemental and isotope compositions of megacrysts, we had analyzed some of them by micro-XRF on a M4 Tornado (Brucker) at Severtsov Institute of Problems of Ecology and Evolution, Russian Academy of Sciences, in Moscow. This tool makes it possible to map the composition of areas as large as a few centimeters across. The anode was made of Rh. The measurements were carried out at an accelerating voltage of 600 V, current 50 μA, in vacuum up 20 mbar. The maps show that megacrysts do not have either zoning or any other large heterogeneities (Figs. 3a–3d). Other megacrysts were analyzed on a MIRA 3 LMU (Tescan Orsay Holding) scanning electron microscope equipped with an Aztec Energy X (Oxford Instruments Nanoanalysis) energy-dispersive spectroscopic analytical system at the shared research facilities Center for Multielemental and Isotope Studies at Sobolev Institute of Geology and Mineralogy, Siberian Branch, Russian Academy of Sciences, in Novosibirsk. The analysis was conducted at an accelerating voltage of 20 kV, beam current of 1.4 nA, and counting time of 20 s. Studies of the megacrysts under an electron microscope also have not detected any zoning in them (Figs. 3e, 3f), but the margins of the crystals have discernible melt zones with newly formed pyroxene crystals up to a few micrometers long.

Before the further analytical studies, feldspar megacrysts were manually crushed under a binocular and hand-picked to get rid of admixtures of the volcanic rock and melt veinlets and margin fragments.

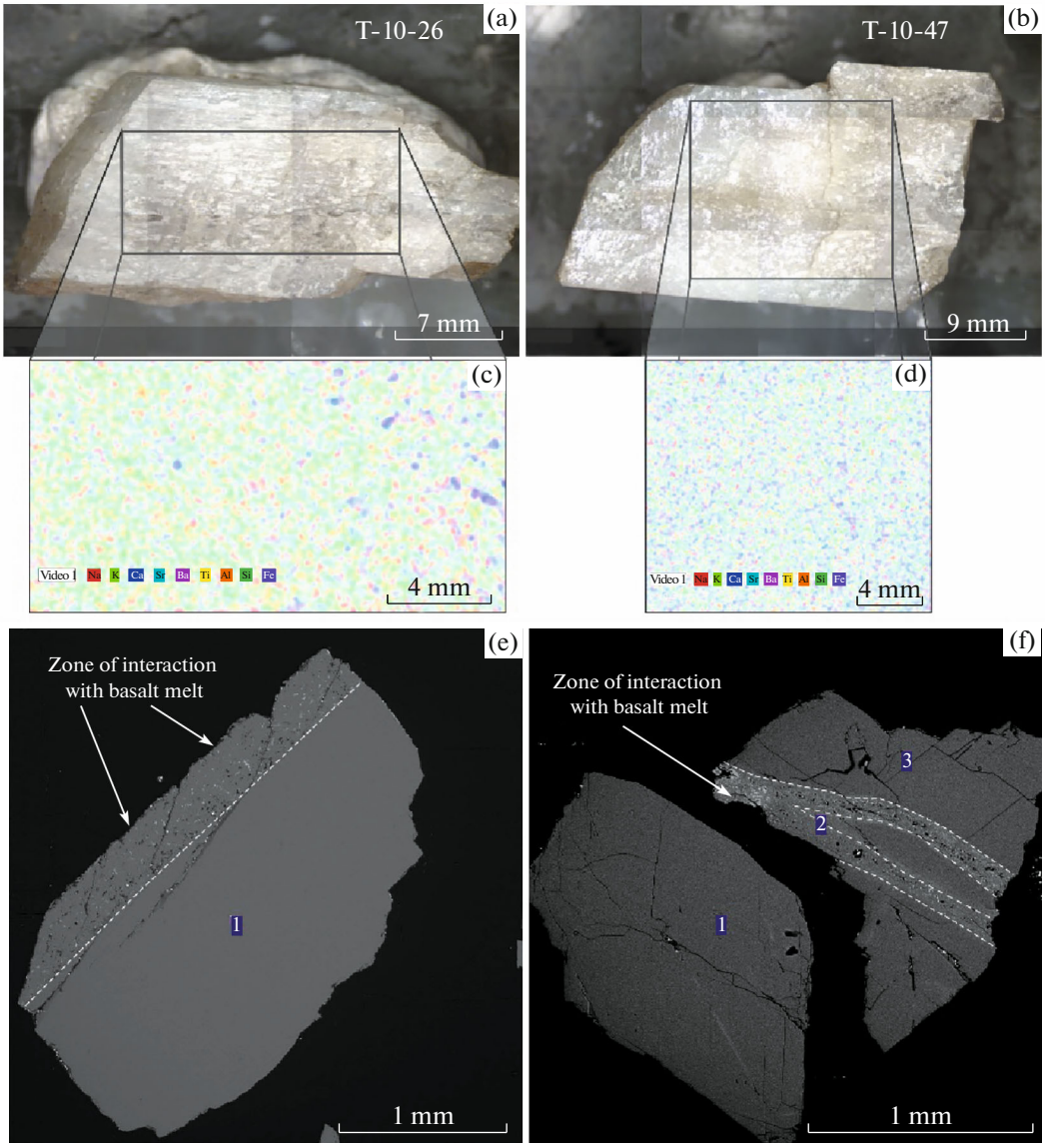

Fig. 3. (a, b) Photo of two samples of feldspar megacrysts from lava flows of Tumusun volcano, Khamar-Daban volcanic field. (c, d) Maps of the distributions of major elements (Na, K, Ca, Sr, Ba, Ti, Al, Si, and Fe) in the two samples. The color codes of the elements are specified in the rectangles below the maps. The maps are drawn based on the micro-XRF data obtained on a M4 Tornado (Brucker) spectrometer. (e, f) BSE images of the feldspars obtained using a scanning electron microscope.

Some of the crystals were then powdered for the isotope studies, whereas analysis for elements was conducted on crystal fragments mounted in epoxy, by the local methods of analysis. All analytical data are summarized in Tables 1–4.

Major components were analyzed in feldspar megacrysts on a CAMEBAX-Micro (Cameca) microprobe at shared research facilities Center for Multielemental and Isotope Studies at Sobolev Institute of Geology and Mineralogy, Siberian Branch, Russian Academy of Sciences, in Novosibirsk. The analysis was conducted at an accelerating voltage of 20 kV, beam current of 40 nA, and counting time of 10 s (analyst O.S. Khmel'nikova).

Feldspars were analyzed for trace elements at the same shared research facilities by LA-ICP-MS. Ablation was done with a Nd: YAG UP-213 (New Wave Research) solid-state laser with a wavelength of 213 nm. The measurements were carried out on an ELEMENT (Thermo Scientific). The carrier gas at ablation in the cell was He, which was mixed with Ar (1 : 4) before letting it into the plasma. Before each of the analytical series, the gas flow was adjusted to reach the maximum intensity of the analytical signals of the elements to analyze. All measurements were done at the maximum frequency of the laser pulse (20 Hz). The detection limits of elements were evaluated from the variations in the signal of the sample-carrying gas. If

Table 1. Representative chemical analyses of feldspar megacrysts from the Khamar-Daban, Iya–Uda, and Vitim volcanic fields

Component	The volcano Tumusun, Khamar-Daban volcanic field							Iya–Uda volcanic field	
	T-10-23/3a	T-10-26/2	T-10-47/2	T-10-50/3	T-10-73/1	T-10-85/3	T-10-97/12	IU-10-8VI	IU-10-8V
FeO	0.13	0.12	0.13	0.13	0.16	0.12	0.11	0.19	0.18
Na_2O	7.05	8.31	8.61	8.49	8.23	7.81	8.89	8.32	8.19
SiO_2	66.9	63.7	67.0	66.2	63.8	64.3	67.4	62.0	61.5
Al_2O_3	21.0	21.5	19.9	20.3	21.3	20.5	19.8	23.7	23.3
CaO	1.2	2.2	0.7	0.8	2.2	1.3	0.4	4.6	4.6
K_2O	3.2	3.0	4.0	4.2	3.0	4.4	4.2	1.1	1.1
BaO	b.d.l.	0.35	b.d.l.	0.09	0.32	0.26	b.d.l.	0.12	0.15
SrO	0.05	0.63	0.11	0.36	0.63	0.85	b.d.l.	0.29	0.44
Total	99.5	99.8	100.4	100.5	99.6	99.6	100.9	100.3	99.4
An	7	11	3	4	11	6	2	22	22
Or	21	17	23	24	17	25	23	6	6
Ab	72	72	74	72	72	68	75	72	72
Ca	8576	15509	5060	5896	15652	9220	3159	33019	32518
Ti	64	134	131	71	218	144	19	221	232
Rb	12	14	42	12	32	26	17	1.7	2.4
Sr	1650	6884	2228	1938	8393	7862	308	6077	8265
Y	0.05	0.15	0.08	0.03	0.17	0.14	0.06	0.20	0.32
Zr	0.21	0.09	0.56	0.08	0.82	0.73	0.05	0.62	2.4
Nb	0.02	0.02	0.19	0.005	0.13	0.13	0.02	0.04	0.13
Cs	0.002	0.004	0.07	0.004	0.02	0.01	0.01	0.02	0.09
Ba	608	4083	985	707	3856	3249	257	2717	4042
La	2.48	9.84	0.90	0.85	9.76	3.11	1.03	13.58	18.35
Ce	2.84	10	1.13	0.92	11	3.38	0.95	20	28
Pr	0.15	0.64	0.08	0.06	0.72	0.21	0.04	1.72	2.27
Nd	0.36	1.48	0.20	0.12	1.85	0.53	0.10	5.30	6.63
Sm	0.03	0.10	0.03	0.02	0.14	0.04	0.01	0.40	0.50
Eu	1.12	1.90	0.55	0.41	3.43	1.42	0.41	1.55	2.07
Tb	0.002	0.002	0.002	0.001	0.01	0.003	b.d.l.	0.01	0.01
Dy	0.02	0.02	0.01	0.002	0.01	0.01	b.d.l.	0.05	0.06
Ho	0.002	0.002	0.002	0.001	0.004	0.001	b.d.l.	0.005	0.01
Er	b.d.l.	0.01	0.002	0.001	0.01	0.001	b.d.l.	0.00	0.02
Tm	b.d.l.	b.d.l.	0.002	0.001	b.d.l.	0.001	b.d.l.	0.002	0.005
Yb	0.002	0.01	0.01	0.001	0.01	0.003	b.d.l.	0.01	0.02
Lu	0.002	0.002	0.002	b.d.l.	0.004	0.001	b.d.l.	0.002	0.003
Hf	0.03	0.04	0.05	0.02	0.08	0.06	0.02	0.14	0.08
Ta	0.07	0.15	0.14	0.07	0.20	0.14	0.05	0.05	0.08
Pb	3.0	5.4	3.5	1.47	6.1	2.6	1.85	8.3	10.5
Th	0.01	0.002	0.02	0.002	0.01	0.01	0.001	0.04	0.01
U	0.004	0.002	0.019	0.001	0.021	0.005	0.002	0.005	0.01

Table 1. (Contd.)

Component	Iya–Uda volcanic field			The volcano Kandidushka, Vitim volcanic field				
	IU-10-IV	IU-10-8II	IU-10-8I	Kand1	Kand2	Kand3	Kand4	Kand5
FeO	0.22	0.23	0.20	0.12	0.13	0.12	b.d.l.	0.12
Na_2O	7.19	6.54	8.46	8.02	8.06	8.20	2.40	8.02
SiO_2	59.4	60.9	62.3	67.1	66.2	66.0	64.9	67.1
Al_2O_3	25.4	24.6	23.3	20.5	20.2	20.4	18.8	20.5
CaO	6.8	5.5	4.4	1.2	1.0	1.0	0.1	1.2
K_2O	0.6	1.0	1.3	4.0	4.5	4.4	13.2	4.0
BaO	b.d.l.	0.07	0.17	b.d.l.	b.d.l.	b.d.l.	0.15	b.d.l.
SrO	0.34	0.39	0.22	0.05	0.20	0.16	b.d.l.	0.05
Total	100.0	99.3	100.4	101.0	100.2	100.2	99.5	101.0
An	33	30	21	6	5	5	0	6
Or	4	6	7	23	26	25	78	27
Ab	63	64	72	71	70	70	22	68
Ca	48670	39451	31232	8219	7040	7218	393	8219
Ti	598	339	243	164	225	185	11	225
Rb	4.5	2.0	2.7	3.4	6.2	7.2	38	3.7
Sr	6706	6577	4596	766	1819	2054	104	1047
Y	0.60	0.31	0.52	0.01	0.13	0.01	0.02	0.01
Zr	6.0	2.0	3.6	0.04	0.79	0.07	0.88	b.d.l.
Nb	0.80	0.23	0.30	0.01	0.24	0.09	0.08	0.004
Cs	0.37	0.02	0.08	0.002	0.05	0.01	0.09	0.002
Ba	1068	1764	2711	68	176	195	264	140
La	5.29	8.49	11.85	0.31	0.78	0.49	0.03	0.25
Ce	10	14	18	0.41	1.1	0.66	0.06	0.33
Pr	1.02	1.17	1.72	0.03	0.13	0.05	0.00	0.02
Nd	3.81	3.72	4.62	0.09	0.39	0.16	0.01	0.10
Sm	0.42	0.42	0.41	0.02	0.07	0.03	0.01	0.02
Eu	0.85	1.09	1.36	0.20	0.32	0.37	0.13	0.21
Tb	0.03	0.02	0.02	b.d.l.	0.01	b.d.l.	0.0005	b.d.l.
Dy	0.12	0.09	0.15	0.002	0.12	b.d.l.	0.003	b.d.l.
Ho	0.03	0.01	0.02	0.002	0.01	b.d.l.	0.001	b.d.l.
Er	0.07	0.03	0.07	0.002	0.03	0.002	0.002	b.d.l.
Tm	0.01	0.004	0.01	0.002	0.002	b.d.l.	0.0005	b.d.l.
Yb	0.05	0.02	0.05	b.d.l.	0.02	0.002	0.001	b.d.l.
Lu	0.01	0.01	0.01	b.d.l.	0.002	b.d.l.	0.0005	b.d.l.
Hf	0.20	0.07	0.10	0.01	0.04	0.02	0.03	0.01
Ta	0.04	0.03	0.07	0.02	0.03	0.03	0.05	0.03
Pb	4.9	5.1	9.2	1.26	4.3	2.0	11.9	0.69
Th	0.23	0.12	0.15	0.01	0.22	0.01	0.003	b.d.l.
U	0.05	0.02	0.05	0.002	0.03	b.d.l.	0.001	b.d.l.

b.d.l. means concentrations below the detection limits, oxides are in wt %, trace elements are in ppm, and end-member of minerals are in mol %.

Table 2. Chemical composition of basalts with megacrysts in the Khamar-Daban, Iya–Uda, and Vitim volcanic fields

Component	Volcanic fields						
	The volcano Tumusun, Khamar-Daban field					The volcano Kandidushka, Vitim volcanic field	Iya–Uda field
	T-10-26	T-10-28	T-10-47	T-10-85	T-10-97	KN-23	IU-10-8
SiO_2	46.2	46.36	45.02	46.83	48.03	44.14	50.66
TiO_2	2.26	2.05	2.56	2.71	2.37	2.38	1.86
Al_2O_3	15.3	14.64	14.74	16.02	14.78	13.20	16.27
Fe_2O_3	2.55	3.60	2.42	2.24	1.82	2.98	1.67
FeO	8.62	7.18	9.7	9.52	9.34	11.25	7.58
MnO	0.172	0.169	0.164	0.161	0.16	0.09	0.13
MgO	8.62	10.2	9.29	7.08	8.24	8.49	6.36
CaO	8.81	8.84	8.48	8.36	8.77	9.14	7.01
Na_2O	3.83	3.76	3.82	3.71	3.35	4.20	4.03
K_2O	1.99	1.76	1.92	2.01	1.47	2.68	2.17
P_2O_5	0.59	0.52	0.58	0.63	0.42	0.75	0.73
LOI	1.06	0.93	1.12	0.84	1.41	0.93	1.23
Total	99.97	100.01	99.81	100.11	100.15	100.23	99.70
FeO*	10.9	10.4	11.9	11.5	10.9	13.9	9.1
Mg#	64.5	61.4	65.3	65.5	66.2	65.0	65.8
$Na_2O + K_2O$	5.82	5.52	5.74	5.72	4.82	6.88	6.20

Oxides are in wt %. Data on the volcano Kandidushka were compiled from (Litasov and Taniguchi, 2002). The values of Mg# and FeO* were calculated as follows: $FeO^* = Fe_2O_3 \times 0.89 + FeO$; $Mg\# = MgO/24.305/(FeO^*/55.845 + MgO/24.305) \times 100$.

Table 3. Compositions of minerals used for the fractional crystallization model

Mineral	SiO_2	TiO_2	Al_2O_3	FeO	Fe_2O_3	MgO	CaO	Na_2O	K_2O
Ano	65.50	–	21.00	–	–	–	1.00	8.25	4.25
Prx	48.78	1.71	10.11	7.05	–	15.01	14.86	1.08	–
TiMt	–	14.5	5.00	58.0	20.0	2.50	–	–	–
Ol (*Fo*-0.88)	40.00	–	–	7.50	–	52.50	–	–	–

Oxides are in wt %. Mineral symbols: *Ano*—anorthoclase, *Prx*—pyroxene *TiMt*—titanomagnetite, *Ol*—olivine.

probable molecular overlaps on the analyzed mass were expected, the mass spectrometer was used in a high-resolution mode. If more than one isotope of an analyzed element occurred, the calculations were done with averaged data on several isotopes. Therewith the number of the replicate measurements increased, while the analytical inaccuracies were reduced. Concentrations of elements in the samples were calculated using an external calibration on the glass standard NIST-612. The data were calibrated against Ca concentration analyzed with the microprobe.

Strontium isotope ratios were measured at the shared research facilities Center for Geodynamics and Geochronology at the Institute of the Earth's Crust, Siberian Branch, Russian Academy of Sciences in Irkutsk, on a Finnigan MAT 262 mass spectrometer. Before the measurements, the powdered material (20–50 mg) of mineral or 100 mg of the basalt were decomposed by HNO_3–HF–$HClO_4$ mixture in Teflon vials placed into a microwave furnace. Strontium was separated from the dissolved sample using Sr Spec (EIChroM Industries, II. USA) resin using HNO_3 of various concentration (Pin et al., 1994). Strontium was recovered by H_2O (Demonterova and Maslovskaya, 2003). The blank was <1 ng Sr. The operation of the system was controlled by replicate measurements of the SRM-987 standard. During this study, the values obtained for the SRM-987 standard were 0.710242 ± 0.000005 (2σ, $n = 8$).

Table 4. Isotope compositions ($\delta^{18}O$‰ and $^{87}Sr/^{86}Sr$) of basalts hosted megacrysts and megacrysts themselves from the Khamar-Daban, Iya–Uda, and Vitim volcanic fields

Sample	Rock/mineral	$\delta^{18}O$ ‰ V-SMOW	SiO_2	$^{87}Sr/^{86}Sr \pm 2\sigma$
IU-10-8	Basalt(groundmass)	7.1	50.66	0.705010 ± 10
KN-23	Basalt (groundmass)	6.2	44.14	0.704228*
T-10-26	Basalt (groundmass)	7.1	46.20	0.704024 ± 12
T-10-28	Basalt (groundmass)	6.7	46.36	0.704180 ± 10
T-10-47	Basalt (groundmass)	6.0	45.02	0.703873 ± 11
T-10-85	Basalt (groundmass)	6.5	46.83	0.703890 ± 10
T-10-85/1	Olivine phenocrysts in basalt	5.8	46.83	0.70389**
T-10-97	Basalt (groundmass)	7.0	48.03	0.704430 ± 12
T-10-97/1	Olivine phenocrysts in basalt	5.8	48.03	0.70443**
T-10-23/3a	Anorthoclase	7.4	46.20	0.704000 ± 12
T-10-26/2	Anorthoclase	7.0	46.20	0.704035 ± 12
T-10-47/2	Anorthoclase	7.6	45.02	0.703837 ± 13
T-10-50/3	Anorthoclase	7.5	45.02	0.703853 ± 16
T-10-73/1	Anorthoclase	7.4	45.02	0.704175 ± 13
T-10-85/3	Anorthoclase	6.9	46.83	0.703938 ± 12
T-10-97/12	Anorthoclase	7.2	48.03	0.704043 ± 15
IU-10-8VI	Plagioclase	8.6	50.66	0.705208 ± 14
IU-10-8VI	Plagioclase	8.9	50.66	0.705286 ± 13
IU-10-8IV	Plagioclase	8.7	50.66	0.705300 ± 12
IU-10-8II	Plagioclase	8.8	50.66	0.705103 ± 10
IU-10-8I	Plagioclase	8.7	50.66	0.705045 ± 14
Kand-1	Anorthoclase	7.5	44.14	0.704000 ± 12
Kand-2	Anorthoclase	6.8	44.14	0.704008 ± 16
Kand-3	Anorthoclase	7.0	44.14	0.704228 ± 13
Kand-4	Sanidine	9.7	44.14	0.711605 ± 14
Kand-5	Anorthoclase	6.9	44.14	0.703999 ± 13

* Data on the volcano Kandidushka are from (Litasov and Taniguchi, 2002); ** value assumed for the host basalt.

The data on $\delta^{18}O$ were obtained on a MAT 253 (Thermo, Germany) mass spectrometer by the laser fluorination technique. The measurements were conducted using double inlet. The measurements were carried out at the shared research facilities Center for Mineralogical and Geochemical Studies at Dobretsov Geological Institute, Siberian Branch, Russian Academy of Sciences, in Ulan-Ude. The measurements were conducted using material that consisted of fragments (1.0–1.5 mm, about 2 mg) of the same phenocryst. If feldspar megacryst was hosted in a fresh rock (except megacrysts in the tuff of Tumusun), the analogous portion (0.5–0.25 mm) of the aphyric basalt was analyzed. Two of the basalt samples contained olivine phenocrysts, which were also analyzed. The measurement results were calibrated in the VSMOW international scale, using two internationally certified standards: NBS-28 (quartz) and NBS-30 (biotite).

RESULTS

General Characterization of Megacrysts and Lavas

In the classification diagram of Fig. 4, the composition of plagioclase from the Iya–Uda volcanic field ranges from oligoclase to andesine: $Ab_{64-72}Or_{4-10}An_{21-33}$. The insignificant scatter of the composition points in Fig. 4 shows that plagioclase megacrysts are highly homogeneous. Volcanic rocks in the area between Iya–Uda rivers vary from basalt and trachybasalt to trachyandesite (Figs. 5a, 5b). The lava hosting megacrysts is basaltic trachyandesite (mugearite): SiO_2 = 50.6 wt %; $Na_2O + K_2O$ = 6.2 wt %; Na_2O/K_2O = 1.86, and Mg# = 59.5 (Figs. 5a, 5b).

Feldspar from the volcano Tumusun in the Khamar-Daban volcanic field is anorthoclase of little varying composition: $Ab_{64-75}Or_{17-28}An_{2-11}$ (Fig. 4). The insignificant scatter of the composition points in

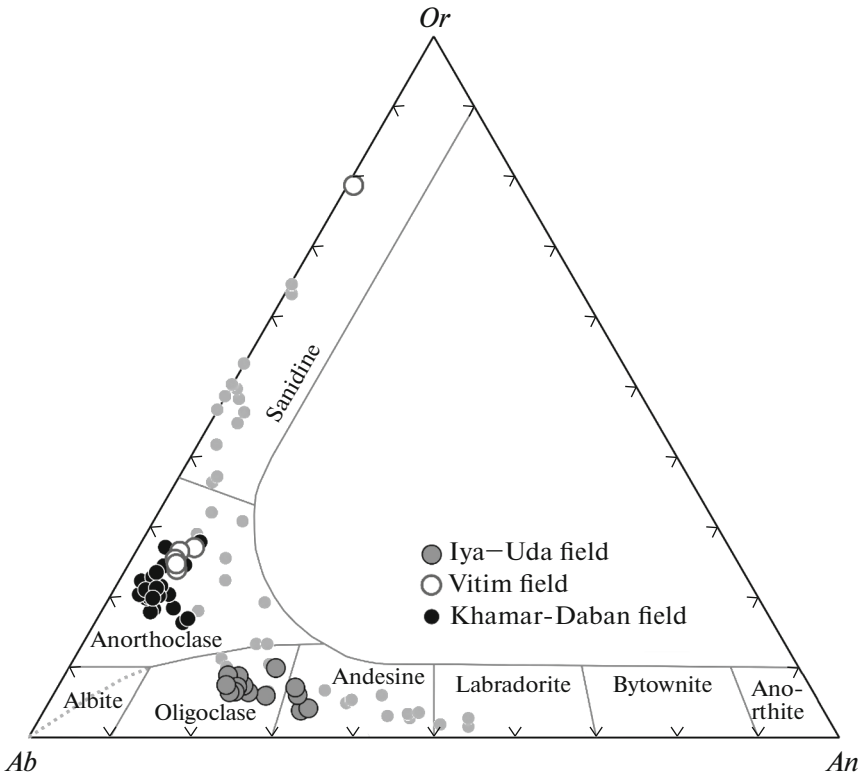

Fig. 4. Classification diagram (Deer et al, 1962–1965) for feldspar megacrysts from the volcano Kandidushka in the Vitim volcanic field, the volcano Tumusun in the Khamar-Daban volcanic field, and a lava flow in the Iya–Uda volcanic field. Small gray circles show the compositions of plagioclase in lherzolite nodules in the Khamar-Daban field (Ionov et al., 1995).

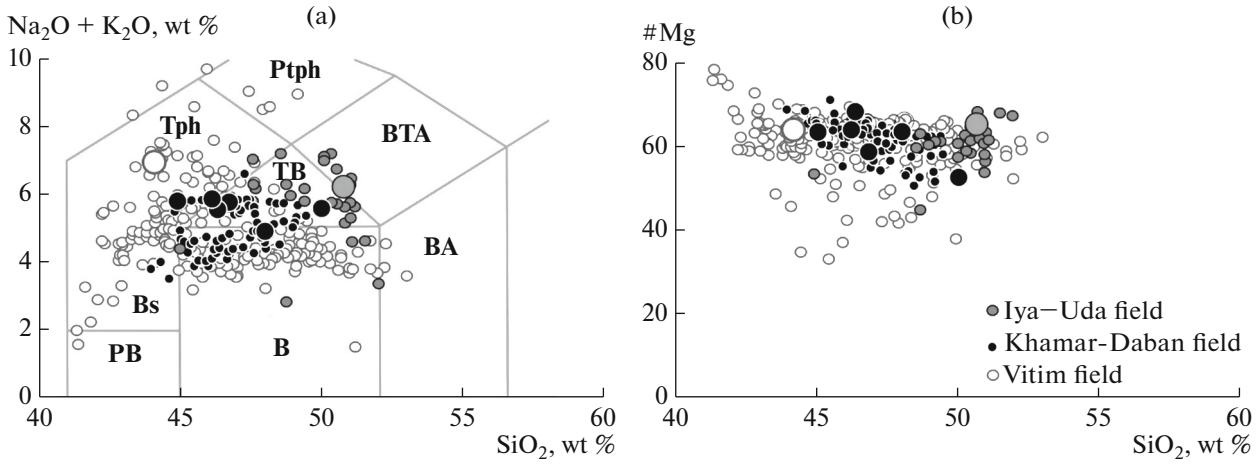

Fig. 5. (a) Total alkalis–silica classification diagram (*Classification of Magmatic Rocks...,* 1997) and (b) SiO_2–Mg# variations for volcanic rocks of the three fields of the Baikal rift zone. The composition of lavas of the Iya–Uda and Khamar-Daban volcanic fields is according to our data, and the composition of lavas in the Vitim volcanic fields are according to our data and those from (Rasskazov, 1993; Litasov and Taniguchi 2002). Large symbols show the chemical composition of basalts with feldspar megacrysts (Table 2). The color of the symbols corresponds to the symbols for the volcanic fields.

Fig. 4 testifies that anorthoclase phenocrysts are compositionally homogeneous, which is consistent with the compositional mapping data and data obtained using a scanning electron microscope (Fig. 3). For comparison, Fig. 4 displays the composition of feldspars from plagioclase-bearing lherzolite nodules in the Khamar-Daban volcanic field. The composition of feldspars broadly varies from andesine to sanidine (Ionov et al., 1995). The lavas entraining megacrysts are basanites and trachybasalts: SiO_2 = 45.0–46.8 wt %;

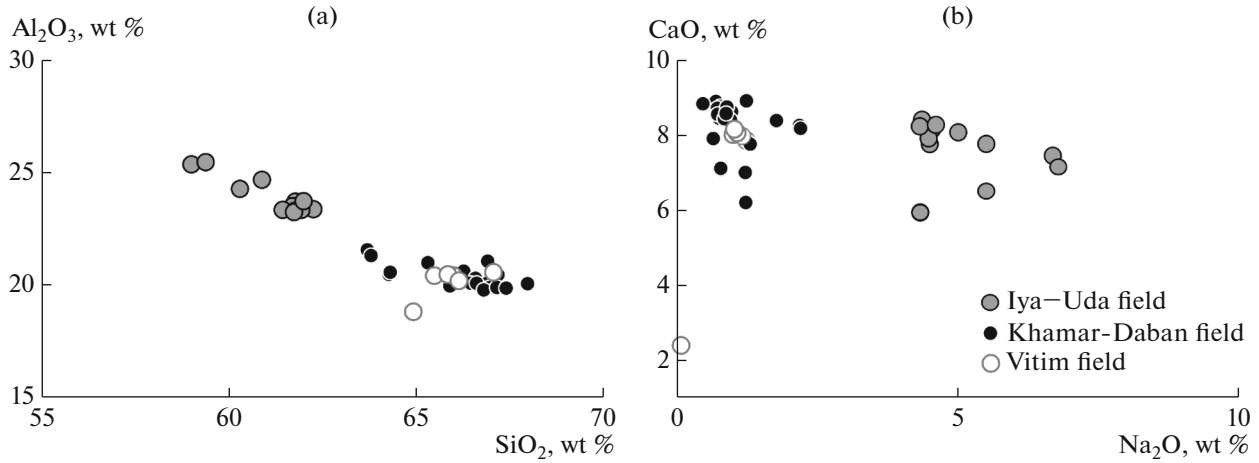

Fig. 6. (a) Al_2O_3–SiO_2 and (b) CaO–Na_2O diagrams for feldspar megacrysts from the volcano Kandidushka in the Vitim volcanic field, the volcano Tumusun in the Khamar-Daban volcanic field, and the Iya–Uda volcanic field.

$Na_2O + K_2O$ = 5.5–5.8 wt %; Na_2O/K_2O = 1.8–2.1, Mg# = 56.3–67.2) (Figs. 5a, 5b).

Most megacrysts from the cinders of the volcano Kandidushka in the Vitim volcanic field plot within the anorthoclase composition field in the classification diagram: $Ab_{54–75}Or_{21–41}An_{5–6}$ (Fig. 4). Megacrysts are compositionally homogeneous, as seen from the insignificant scatter of their composition points. We have found one sanidine ($Ab_{22–78}$) crystal in the cinders. The cinders and lava flow correspond to basanite: SiO_2 = 43.9–45.5 wt %; $Na_2O + K_2O$ = 6.8–7.4 wt %; Na_2O/K_2O = 1.5–1.6, Mg# = 56.1–60.8 (Ashchepkov, 1991; Litasov and Taniguchi, 2002) (Fig. 5).

Variations in Concentrations of Major Components and Trace Elements in Feldspars

The variability of the major-component composition of feldspar megacrysts is illustrated in Fig. 6 by (a) Al_2O_3–SiO_2 and (b) CaO–Na_2O diagrams. Andesine and oligoclase from the Iya–Uda volcanic field are the most sodic, with high Al_2O_3 and low SiO_2 and K_2O concentrations. Megacrysts from the Vitim and Khamar-Daban fields are compositionally similar. The only exception is sanidine from the volcano Kandidushka. It should be mentioned that the composition of the feldspar megacrysts broadly varies even within a single lava flow, such as in the Iya–Uda volcanic field or the volcano Kandidushka.

The chondrite-normalized multielemental patterns of all of feldspars have positive Eu anomalies (Fig. 7a). High REE concentrations are typical of plagioclase from the Iya–Uda volcanic field, whereas these elements are depleted in sanidine form the volcano Kandidushka. Anorthoclase megacrysts from Kandidushka in the Vitim field and Tumusun in the Khamar-Daban field have similar HREE patterns. At the same time, anorthoclase from the volcano Tumusun is richer in LREE than this mineral from the volcano Kandidushka. The primitive mantle-normalized multielemental patterns of all of phenocrysts show positive Ba, Sr, and Pb anomalies and negative ones of Th, U, Pr, Nb, Zr, and Hf (Fig. 7b). It can be also seen that, having many features in common with the other megacrysts, megacrysts of plagioclase from the Iya–Uda volcanic field are noted for higher concentrations of trace elements. Sanidine from the volcano Kandidushka is richer in Rb, Ta, Pb, Zr, and Hf than the other megacrysts but contains the lowest La, Ce, Pr, and Sr concentrations.

Variations in $\delta^{18}O$ and $^{87}Sr/^{86}Sr$ of the Lavas and Feldspar Megacrysts

Unlike the analysis of the variations of radiogenic isotopes, the variations of stable isotopes should be analyzed with regard to their fractionation between the melt and crystallizing phases. This effect can be provisionally evaluated, although uncertainties of the order of a few tenths of a pro mille remain depending on the assumed model, mineral–melt fractionation coefficient, H_2O and CO_2 degassing from the magma, etc. (Eiler, 2001; Zhao and Zheng, 2003; Vho et al., 2020). Figure 8 shows relationships between the $\delta^{18}O$ of minerals and their host rocks. It is seen that all plagioclase megacrysts from the Iya–Uda volcanic field and sanidine from the Vitim volcanic field (the volcano Kandidushka) plot away from the theoretical mineral–melt equilibrium lines toward higher $\delta^{18}O$ values, whereas many of anorthoclase megacrysts have lower $\delta^{18}O$ values. As was pointed out above, the exact location of the fractionation line depends on several factors. However, the scatter of the data points is too large to be explained only by the isotope fractionation. This scatter indicates, first of all, that feldspar megacrysts were not

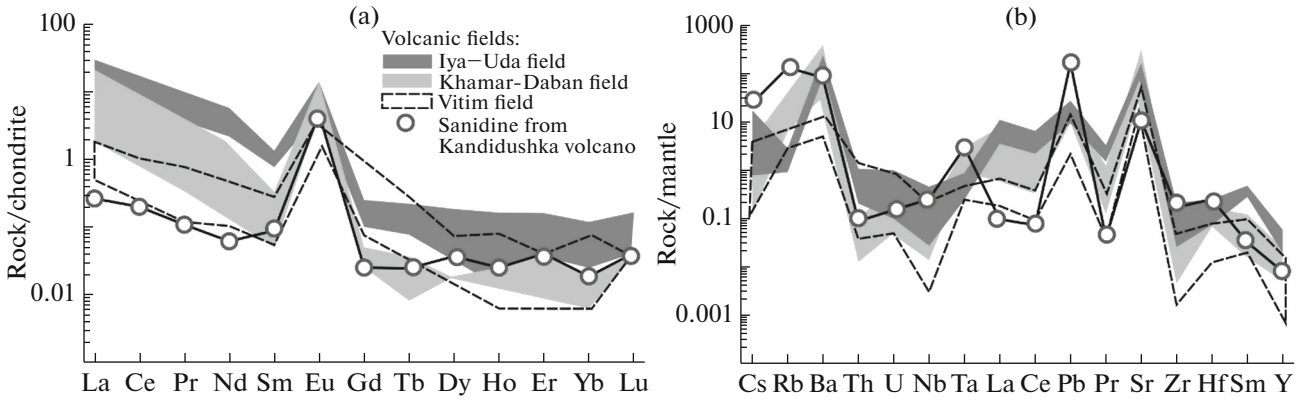

Fig. 7. (a) Chondrite-normalized (McDonough and Sun, 1995) and (b) primitive mantle-normalized (Sun and McDonough, 1989) REE patterns of feldspar megacrysts.

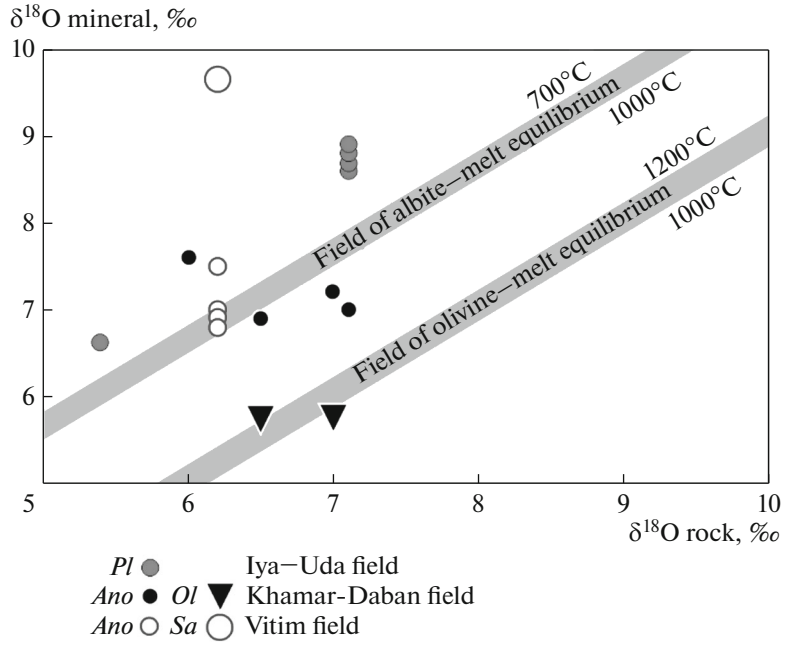

Fig. 8. Relationships between the $\delta^{18}O$ of minerals and their host rocks. Gray fields show theoretical relations for the equilibrium crystallization of olivine (*Ol*) at temperatures of 1200–1000°C and albite (*Ab*) with 30% of anorthite end-member at temperatures of 1000–700°C from basalt melt (Zhao and Zheng, 2003). Provisionally, albite most closely, among *Or–Ab–An* feldspars, approximates the isotope fractionation of anorthoclase and plagioclase (Fig. 4).

in oxygen isotope equilibrium with the melt that entrained them. This means that, in the strict sense, megacrysts are in fact antecrysts. Second, the general shift of the $\delta^{18}O$ values of minerals toward lower $\delta^{18}O$ values from the equilibrium line suggests that the crystal grew in a more primitive magma than that entraining it. The shift of the $\delta^{18}O$ values of feldspars from the equilibrium line toward higher $\delta^{18}O$ values indicates that mineral crystallized from melt that either had got a lower temperature or was contaminated by crustal material. The region of higher $\delta^{18}O$ values includes the composition points of some anorthoclase megacrysts and the points of all plagioclases and sanidine. The variations in the oxygen isotope composition of olivines are consistent with its equilibrium crystallization in melt within the temperature range of 1200–1000°C.

An analogous conclusion that feldspar megacrysts were not in equilibrium with melts that entrained them follows from analysis of Sr isotope ratios (Fig. 9a). Almost all plagioclases from the Iya–Uda volcanic field possess higher $^{87}Sr/^{86}Sr$ ratios than the rocks hosting these megacrysts, and anorthoclase from the Khamar-Daban (the volcano Tumusun) and Vitim (the volcano Kandidushka) volcanic fields either plots

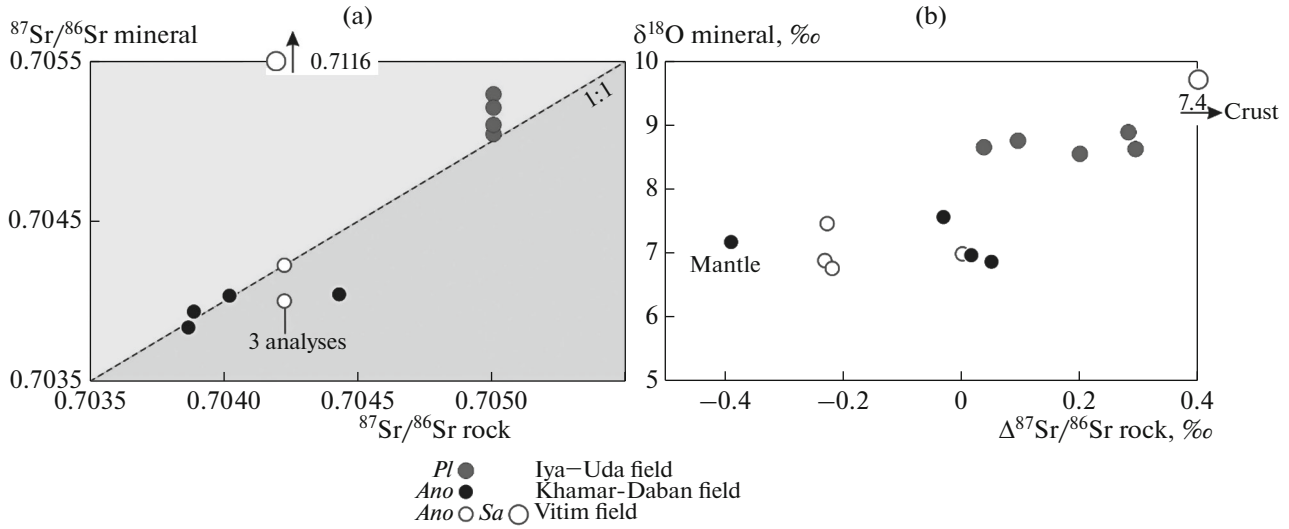

Fig. 9. Diagrams of (a) the $^{87}Sr/^{86}Sr$ ratios of minerals and their host rocks and (b) deviations of the $^{87}Sr/^{86}Sr$ ratios ($\Delta^{87}Sr/^{86}Sr$) from the 1 : 1 line against the $\delta^{18}O$ of feldspars.

near the 1 : 1 line or is notably shifted toward lower $^{87}Sr/^{86}Sr$ compared to the rock (Fig. 9a). This is even more clearly seen in the $\Delta^{87}Sr/^{86}Sr$–$\delta^{18}O$ diagram (Fig. 9b) for feldspars, where $\Delta^{87}Sr/^{86}Sr$ is the deviation of feldspars from the 1 : 1 line in Fig. 9a. All of anorthoclase megacrysts show more "mantle-like" values, whereas plagioclase and sanidine megacrysts are shifted toward "crustal-like" values.

DISCUSSION

When feldspar megacrysts are studied, the question arises of whether minerals could crystallize immediately from the magmas entraining them or from magmas of similar composition. It has been demonstrated (Guo et al., 1992; Perini, 2000; Lundstrom et al., 2005) that this requires compositions close to trachyte and trachyandesite. Lavas of trachyte composition were found in our study area only in the Udokan volcanic field (Rasskazov, 1985; Stupak et al., 2012), although feldspar inclusions have been found in all volcanic fields in Central Asia in rocks of basalt (*sensu lato*) composition. It has been hypothesized (Litasov and Mal'kovets, 1998) that anorthoclase megacrysts can crystallize from high-Si melt that can result from the settling of oxide phases, with crystallization in a magma chamber at medium- to upper-depth levels of the crust. Figure 10 shows the variations in the major-element composition of basalts in the Vitim, Khamar-Daban, and Iya–Uda volcanic fields and the calculated crystallization trends at the differentiation of olivine, clinopyroxene, titanomagnetite, and anorthoclase of constant composition. The compositions of minerals are listed in Table 3 and correspond to those of minerals that crystallized in equilibrium with alkali basalt magmas in experiments (Esin, 1993) and in samples of natural rocks (Rasskazov and Ivanov, 1998). Figure 10 shows that, if anorthoclase crystallized from a more silicic melt, for example, basaltic trachyandesite (T-10-42, Tumusun volcano, Table 2), then the fractional crystallization of about 20% anorthoclase of composition as megacrysts in the Khamar-Daban volcanic field would result in lavas of composition within the range of the Tumusun lavas. The simulations of the contamination of alkali olivine basalt with various crustal components using the MELTS (Edwards and Russell, 1996) software have shown that plagioclase could have crystallized as the first mineral phase. It was also pointed out in the aforementioned publication that granite as a contaminant results in the crystallization of sanidine as an equilibrium feldspar. Data on the petrography of Late Cenozoic basalts in the Baikal rift indicate that anorthoclase is their rock-forming mineral, whose content reaches 15–20% (Yarmolyuk et al., 2003). Hence, petrologic data indicate that feldspar megacrysts could in principle have crystallized in the Baikal region directly from silica-enriched magmas and/or from magmas contaminated by crustal material.

The most popular model is that feldspars are formed by diffusion–reaction processes proceeding between magma and crustal host rocks in intermediate magma chambers (Duffield and Ruiz, 1992; Tepley et al., 2000; Lundstrom et al., 2005; Renjith, 2014; Coote et al., 2018). It is believed that there is a zone where the pressure gradient changes, where basalt melt can reside for a while and undergo assimilation and fractional crystallization (Geist et al., 1988; Tepley et al., 1999; Ivanov, 2012). Therewith feldspars crystallize at boundaries between rocks of various composition and the partly crystallized melt (Lundstrom et al., 2005; Coote et al., 2018). Figure 11 dis-

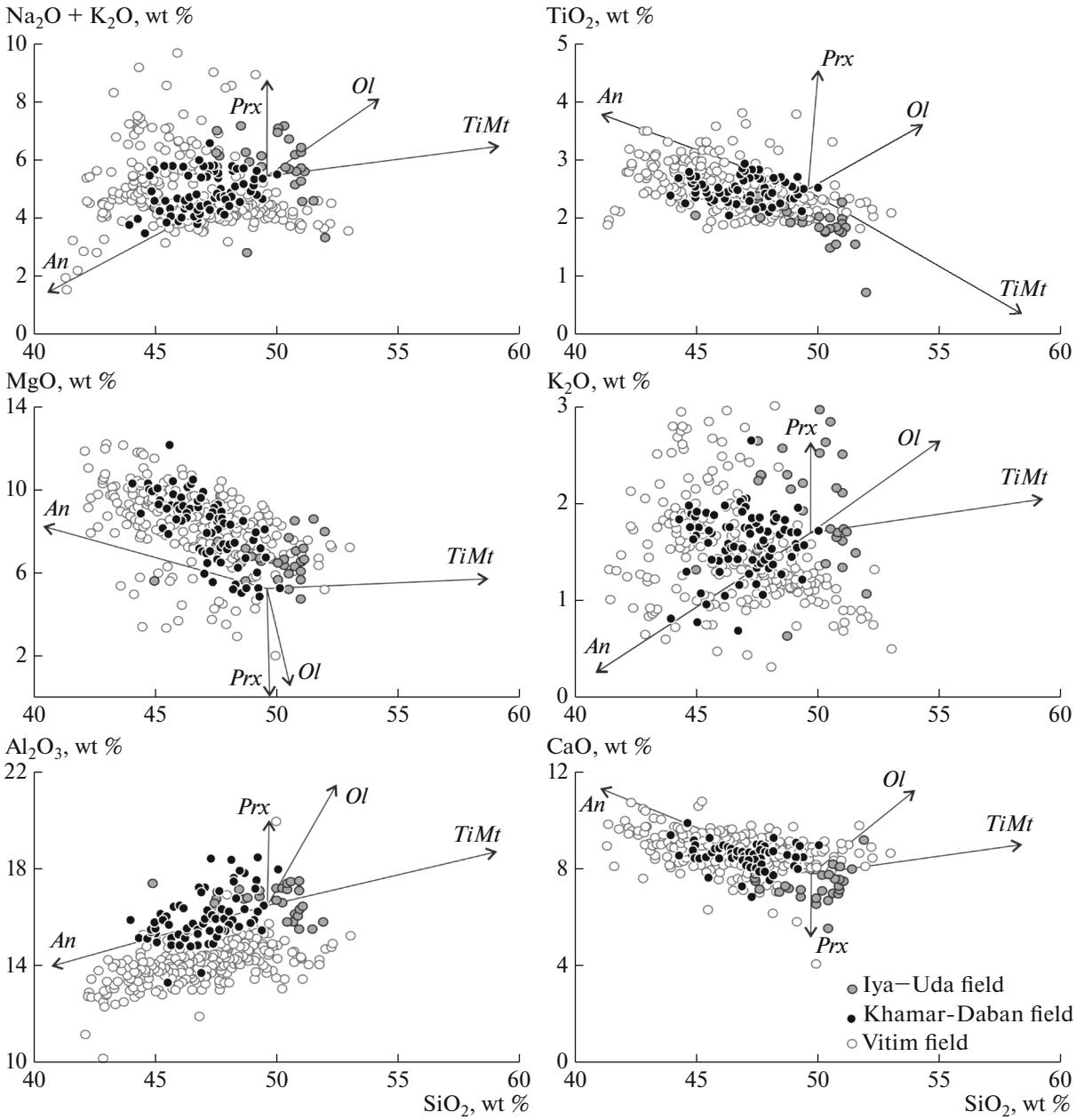

Fig. 10. Variations in concentrations (wt %) of major oxides in volcanic rocks of the Iya–Uda, Khamar-Daban, and Vitim volcanic fields. The composition of lavas of the Iya–Uda and Khamar-Daban volcanic fields are according to our data, and those of the Vitim volcanic field are from (Rasskazov, 1993). Lines show the calculated changes in the chemical composition of the magmas depending on the fractionation of dominant rock-forming minerals and anorthoclase megacrysts. The starting composition is assumed as that of a lava flow of the volcano Tumusun (sample T-10-42, Khamar-Daban volcanic field) and the composition of minerals from Tables 2 and 3.

plays how melts can be stagnated at a crustal level because the density variations in the crust are stepwise, whereas the density of magma varies gradually (Kushiro, 2007; Ivanov, 2012). Thereby "dry" magmas of normal alkalinity can be more probably stagnated than alkaline fluid-rich magmas (Fig. 11). Of course, crustal density profiles may (and do) differ from one region to another, and each region is characterized by its own types of emplaced magmas, which should also control the depths at which the magmas are stagnated. Variations in the isotope composition of feldspars are often interpreted as resulting from crystal growth in a magma chamber replenished with isotopically heterogeneous melt portions and the crustal contamination of these melts (Tepley et al., 2000; Lundstrom, 2005; Higgins and Chandrasekharam, 2007; Renjith, 2014; Sheth, 2016; Coote et al., 2018). Diffusion plays a more important role in the crystallization

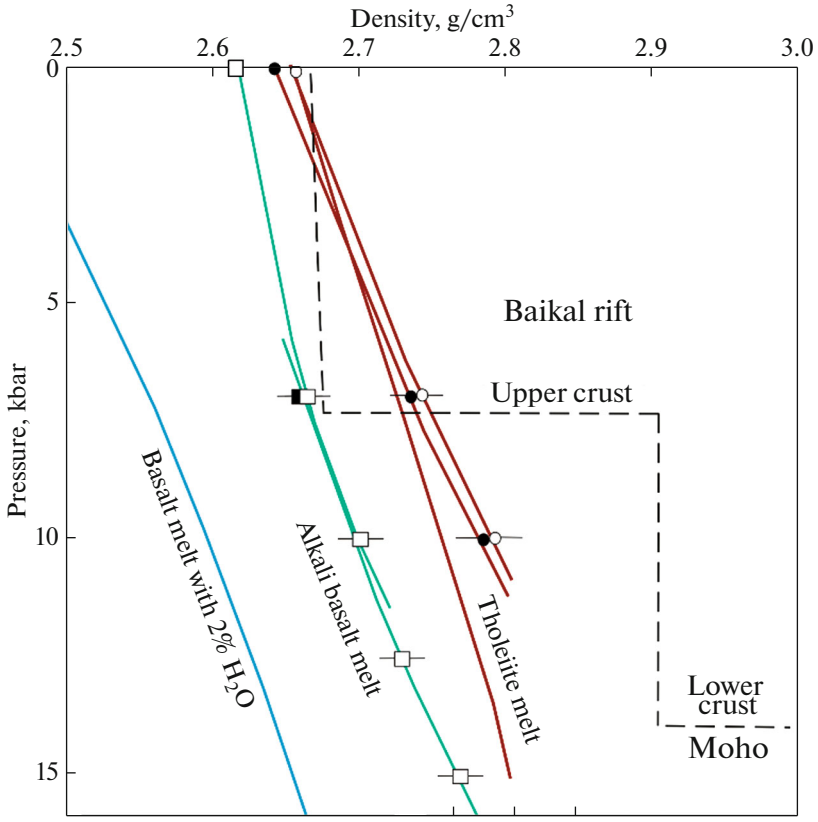

Fig. 11. Density of various mantle-derived melts within the crustal depth range. The heavy dashed line shows the hypothetical density profile of crust in the continental area of the Baikal rift. In both cases, tholeiite melts have a higher density than that of the granitic layer of the crust, whereas alkali basalt and hydrous melts can be stagnated at crustal depths only in thickened crust. This figure is compiled and simplified from (Ivanov, 2012).

of feldspars than at the crystallization of more stable minerals, such as olivine or quartz, but correlations in the behavior of major elements and the Sr isotope system provide a record of the crystallization conditions of feldspars and the history of the magmatic system as a whole (Davidson et al., 2005; Davidson et al., 2007). Megacrysts can crystallize in various parts of magmatic systems and during various stages of the magmatic pulse, but their growth and movements are related to closely genetically interrelated parental magmas but not to older host rocks. The melts should be stagnated and pool to enable large crystals to be formed, whose growth is maintained by new portions of material from the replenished magma (Lundstrom, 2005; Higgins and Chandrasekharam, 2007; Renjith, 2014; Sheth, 2016).

The crystallization conditions of megacrysts and mantle nodules entrained by lavas in the Baikal rift vary within broad P–T ranges of 900–1400°C and 7–35 kbar (Ashchepkov et al., 2011). Proportions of elements in feldspars depend on temperature, pressure, and the composition of the host rocks (Coote et al., 2018; Li et al., 2019). The retainment of melts at phase transitions and/or at changes in the rheology and composition of crustal rocks may result in fracturing of the rocks and the origin of veins and/or the growth of crystals on the wall rocks, with the subsequent detachment of these crystals and their entrainment to the surface (Ashchepkov et al., 2011; Lundstrom et al., 2005).

Variations in the oxygen and strontium isotope compositions of feldspars and rocks that entrain them indicate, on the one hand, that the feldspar megacrysts and the melts hosting them were not in isotope equilibrium. On the other hand, the studied anorthoclase megacrysts evidently (Fig. 9b) crystallized from more primitive magmas with mantle isotope characteristics, whereas the plagioclase crystallized from magmas more significantly contaminated with crustal rocks, and sanidine is likely a xenocryst from crustal rocks. Thus, the origins of feldspar megacrysts were obviously different. Sanidine was captured in the crust. Plagioclase crystallized in a magma chamber at the boundary between the upper and lower crust, from crustally contaminated magma. Anorthoclase crystallized at the greatest depths from primitive magma with mantle isotope characteristics. Figures 12a and 12b schematically render a generalized model for the origin of megacrysts in the Baikal rift. According to this model, the primary partial melts

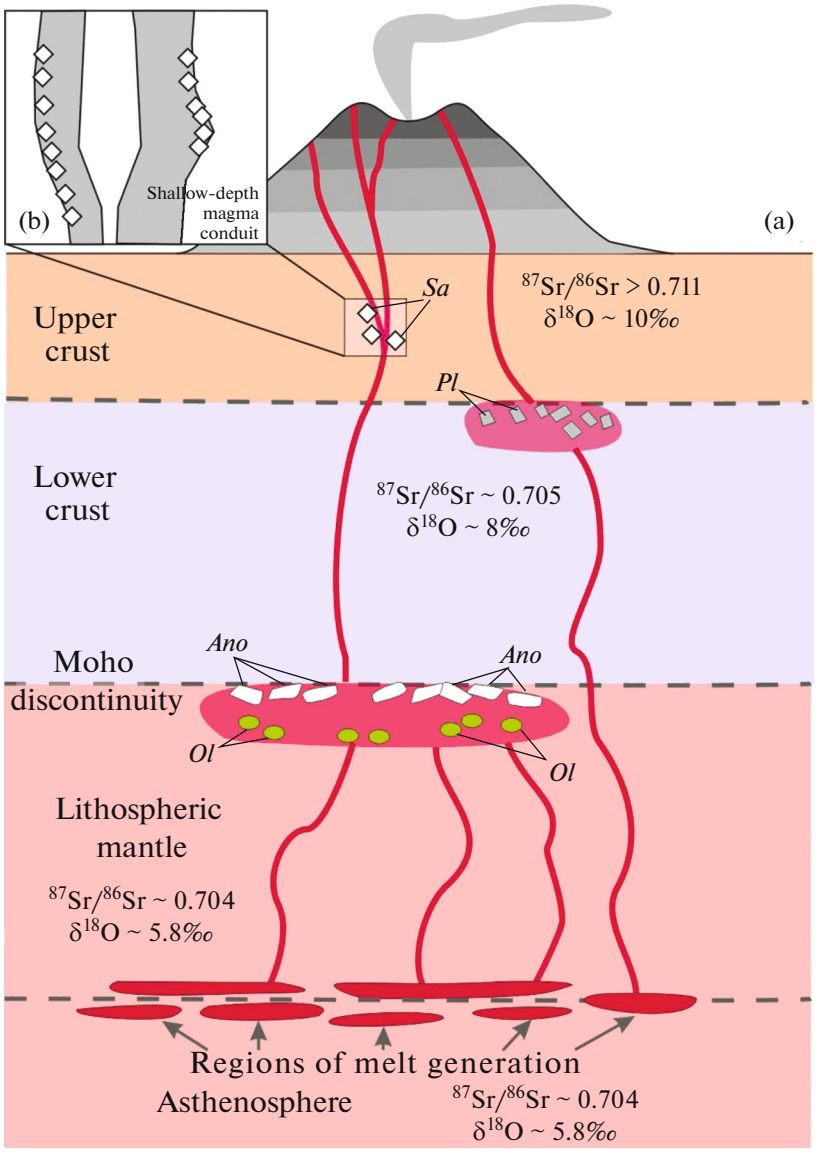

Fig. 12. Schematized and generalized model for the crystallization of feldspar megacrysts in magmas of the Baikal rift. The figure also shows the inferred $^{87}Sr/^{86}Sr$ and $\delta^{18}O$ isotope parameters of the crustal and mantle melting reservoirs. (b) Areas in which sanidine megacrysts may have been formed.

with mantle $^{87}Sr/^{86}Sr$ and $\delta^{18}O$ values ascended to the Moho, where a deep-sitting chamber was formed because the density of the lower crust is lower than that of the magma (Figs. 11, 12a, 12b). Olivine and anorthoclase crystallize from the primary magmas with mantle isotope characteristics. The shape of anorthoclase crystals leads to their flotation and accumulation in the upper part of such deep magma chambers (in principle, there may be more than one such a chamber at various depth levels). The high temperature and chemical homogeneity of the magma precludes the growth of zoned anorthoclase crystals because of the rapid reequilibration of various zones of the mineral. The magma density in the deep magma chamber decreases as a result of olivine crystallization and accumulation. The differentiated and partly contaminated magma entrains anorthoclase crystals to the surface, as was the case with the volcanoes Tumusun and Kandidushka. If the primary melts had densities lower than that of the lower crust, these melts could have reached the lower–upper crust boundary, where the density of the crustal material abruptly changes again (Figs. 11, 12a, 12b). In this relatively shallow-depth magma chamber, the magma may have been contaminated by upper-crustal rocks, and thus the magma composition (first of all, its isotope characteristics) may have significantly changed. This strongly contaminated magma crystallized sodic plagioclase.

Because of its shape and density lower than that of the magma, the plagioclase also buoyantly ascended and was accumulated in the upper part of the magma chamber. This plagioclase was brought to the surface by less contaminated magmas that replenished the chamber. This scenario pertains to the Iya–Uda volcanic field. Finally, the magmas may have captured crustal xenoliths *en route* to the surface.

As seen from the aforesaid, the origin of feldspar megacrysts cannot be explained within the framework of any single universally applicable model. First, the composition of feldspar megacrysts may be different at various volcanic fields, which suggests different crystallization temperatures and pressures. Second, the same lava flow can entrain different feldspars generations of different age. Third, megacrysts differ in inner structure from zoned crystals with inclusions of other minerals to practically unzoned ones, as is the case with the volcanic fields discussed above. Fourth, the Sr isotope composition of megacrysts and their host rocks may either coincide or differ, which depends on the composition of the possible contaminants. Fifth, the large feldspar crystals crystallized not in the magma that entrained them: megacrysts are antecrysts, but at the same time, the lavas and megacrysts are interrelated through a single volcanic cycle.

CONCLUSIONS

Mineralogical and isotope–geochemical variations in feldspar megacrysts and Late Cenozoic lavas, tuffs, and cinders carrying these megacrysts at three volcanic fields of the Baikal rift system reflect both primary variations in the composition of the mantle magmas and the degrees of contamination of the mantle magmas with crustal material. Anorthoclase and plagioclase crystals are actecrysts: they did not crystallize from the magmas that entrained them but are nevertheless related to these magmas within a single volcanic process. Anorthoclase crystallized in the deepest chambers from the most primitive mantle-derived melts, whereas plagioclase crystallized in crustal magma chambers at interaction between the magma and felsic crust. The immediate capture of granitic material may have result in sanidine megacrysts.

ACKNOWLEDGMENTS

The authors thank B.G. Pokrovskii, K.N. Shatagin, and E.O. Dubinina for constructive criticism that led us to significantly improve the manuscript. The studies were carried out at the following shared research facilities: Center for Geodynamics and Geochronology at the Institute of the Earth's Crust, Siberian Branch, Russian Academy of Sciences, in Irkutsk, Center for Multielemental and Isotope Studies at Sobolev Institute of Geology and Mineralogy, Siberian Branch, Russian Academy of Sciences, in Novosibirsk, and the Analytical Center of Mineralogical–Geochemical and Isotope Studies at Dobretsov Geological Institute, Siberian Branch, Russian Academy of Sciences, in Ulan-Ude.

FUNDING

The equipment of the Center for Geodynamics and Geochronology was used in this research under Grant 075-15-2021-682. The fieldwork and EPMA studies were supported by Megagrant 075-15-2022-1100.

CONFLICT OF INTEREST

The authors declare that they have no conflicts of interest.

REFERENCES

A. V. Akinin, A. V. Sobolev, T. Ntaflos, and W. Richter, "Clinopyroxene megacrysts from Enmelen melanephelinitic volcanoes (Chukchi Peninsula, Russia): application to composition and evolution of mantle melts," Contrib. Mineral. Petrol. **150**, 85–101 (2005).

I. V. Ashchepkov, *Deep-Seated Xenoliths of the Baikal Rift* (Nauka, Novosibirsk, 1991) [in Russian].

I. V. Ashchepkov, S. V. Travin, A. I. Saprykin, L. Andre, P. A. Gerasimov, and O. S. Khmelnikova, "Age of xenoith-bearing basalts and mantle evolution in the Baikal rift zone," Russ. Geol. Geophys. **44** (11), 1121–1149 (2003).

I. V. Ashchepkov, L. André, H. Downes, and B. A. Belyatsky, "Pyroxenites and megacrysts from Vitim picrite-basalts (Russia): polybaric fractionation of rising melts in the mantle?," J. Asian Earth Sci. **42**, 14–37 (2011).

V. G. Belichenko, E. V. Sklyarov, and N. L. Dobretsov, "Geodynamic map of the Paleoasian ocean. Eastern segment," Geol. Geofiz. **35** (7–8), 29–40 (1994).

V. G. Belichenko, N. K. Geletii, and I. G. Barash, "Barguzin microcontinent (Baikal mountain area): the problem of outlining," Russ. Geol. Geophys. **47** (10), 1049–1059 (2006).

I. N. Bindeman, V. V. Ponomareva, J. C. Bailey, and J. W. Valley, "Volcanic arc of Kamchatka: a province with high-Δ18O magma sources and large-scale $^{18}O/^{16}O$ depletion of the upper crust," Geochem. Cosmoch. Acta **68**, 841–865 (2004).

M. I. Burakov and E. E. Fedorov, "Basalts of the Iya–Uda interfluve (East Sayan)," *Geological Problems of Asia* (AN SSSR, Moscow, 1954), Vol. 1 [in Russian].

A. Coote, P. Shane, C. Stirling, and M. Reid, "The origin of plagioclase phenocrysts in basalts from continental monogenetic volcanoes of the Kaikohe-Bay of Islands field, New Zealand: implications for magmatic assembly and ascent," Contrib. Mineral. Petrol. **173**, no. 14 (2018).

J. P. Davidson, B. Charlier, and J. M. Perlroth, and R. Hora, "Mineral isochrons and isotopic fingerprinting: pitfalls and promises," Geology **33** (1), 29–32 (2005).

J. P. Davidson, D. J. Morgan, B. Charlier, B. L. A. Charlier, R. Harlou, and J. M. Hora, "Microsampling and Isotopic Analysis of Igneous Rocks: Implications for the

Study of Magmatic Systems," Annu. Rev. Earth Planet. Sci. **35**, 273–311 (2007).

E. I. Demonterova, A. V. Ivanov, and A. B. Perepelov, "Late Cenozoic volcanism of the Uda river area (eastern Sayan, Siberia): the first geochemical and isotopic data," Geodynam. Tectonophys. **8** (3), 445–448 (2017).

E. I. Demonterova and M. N. Maslovskaya, "Chromatographic extraction of strontium in samples with high Rb/Sr ratios for mass-spectrometric analysis," *Applied Geochemistry. Analytical Studies,* Ed. by E. K. Burenkov and A. A. Kremenetskii, (IMGRE, Moscow, 2003), Vol. 4, pp. 15–19. [in Russian].

W. A. Deer, R. A. Howie, and J. Zussman, *Rock-Forming Minerals. Volume 4. Framework Silicates* (Longmans, London, 1963).

N. V. Dmitrieva and A. D. Nozhkin, "Geochemistry of the Paleoproterozoic metaterrigenous rocks of the Biryusa Block, southwestern Siberian Craton," Lithol. Miner. Resour. **47** (2), 156–179 (2012).

T. V. Donskaya, D. P. Gladkochub, A. M. Mazukabzov, and M. T. D. Vingeit, "Early Proterozoic postcollisional granitoids of the Biryusa block of the Siberian Craton," Russ. Geol. Geophys. **55** (7), 1028–1043 (2014).

W. A. Duffield and J. Ruiz, "Compositional gradients in large reservoirs of silicic magma as evidenced by ignimbrites versus Taylor Creek Rhyolite lava domes," Contrib. Mineral. Petrol. **110**, 192–210 (1992).

B. R. Edwards and J. K. Russell, "Influence of magmatic assimilation on mineral growth and zoning," Can. Mineral. **34**, 1149–1162 (1996).

J. M. Eiler, "Oxygen isotope variations of basaltic lavas and upper mantle rocks," Rev. Mineral. Geochem. **43** (1), 319–364 (2001).

S. V. Esin, *Injection Magmatism in the Upper Mantle: Testing Empirical Clinopyroxene Geobarometer* (NITs OIGGM SO RAN, Novosibirsk, 1993) [in Russian].

G. Faur, *Principles of Isotope Geology* (Wiley, 1986).

D. J. Geist, J. D. Myers, and C. D. Frost, "Megacryst–bulk rock isotopic disequilibrium as an indicator of contamination processes: the Edgecumbe Volcanic Field, SE Alaska," Contrib. Mineral. Petrol. **99**, 105–112 (1988).

J. F. Guo, T. H. Green, and S. Y. O'Relly, "Ba partitioning and the origin of anorthoclase megacrysts in basalitic rocks," Mineral. Mag. **56**, 101–107 (1992).

M. D. Higgins and D. Chandrasekharam, "Nature of subvolcanic magma chambers, Deccan Province, India: Evidence from quantitative textural analysis of plagioclase megacrysts in the Giant plagioclase basalts," J. Petrol. **48** (5), 885–900 (2007).

W. Hildreth, "A critical overview of silicic magmatism," in *Penrose Conference on Longevity and Dynamics of Rhyolitic Magma Systems, Mammoth, USA, 2001* (Mammoth, 2001).

D. A. Ionov, S. Y. O'Reilly, and I. V. Ashchepkov, "Feldspar-bearing lherzolite xenoliths in alkali basalts from Hamar–Daban, southern Baikal region, Russia," Contrib. Mineral. Petrol. **122**, 174–190 (1995).

A. V. Ivanov, "Interaction of mantle melts with crust during their ascent to the surface: reason and consequences," Geodinam. Tektonofiz. **3** (1), 19–26 (2012).

A. V. Ivanov, E. I. Demonterova, A. B. Perepelov, V. Lebedev, and H. He, "Volcanism in the Baikal rift: 40 years of active-versus-passive model discussion," Earth-Sci. Rev. **148**, 18–43 (2015).

A. I. Kiselev, M. E. Medvedev, and G. A. Golovko, *Volcanism of the Baikal Rift Zone and Problems of Deep-Seated Magma Formation* (Nauka, Novosibirsk, 1979) [in Russian].

Classification of Igneous Rocks and Glossary of Terms. Recommendations of Subcommision on Systematics of Igneous Rocks of the International Union of Geological Sciences (Nedra, Moscow, 1997) [in Russian].

I. Kushiro, "Origin of magmas in subduction zones: a review of experimental studies," Proc. Japan. Academ., Series B. **83**, 1–15 (2007). https://doi.org/10.2183/pjab.83.1

W. Li, C. Tao, W. Zhang, J. Liu, J. Liang, S. Liao, and W. Yang, "Melt inclusions in plagioclase macrocrysts at Mount Jourdanne, Southwest Indian Ridge (~64° E): implications for an enriched mantle source and shallow magmatic processes," Minerals. **9**, 493 2019).

K. D. Litasov and V. G. Malkovets, "Sr-Ba-Rb–systematics of megacrystals of alkaline feldspars from basaltic rocks of Central Asia," Geol. Geofiz. **39** (9), 1304–1308 (1998).

K. D. Litasov and H. Taniguchi, *Mantle Evolution beneath Baikal Rift*, CNEAS Monogr. Ser. **5**, (2002).

C. Lundstrom, A. Boudreau, and M. Pertermann, "Diffusion–reaction in a thermal gradient: Implications for the genesis of anorthitic plagioclase, high alumina basalt and igneous mineral layering," Earth Planet. Sci. Lett. **237** (3–4), 829–854 (2005). https://doi.org/10.1016/j.epsl.2005.06.026Mc

W. F. McDonough and S. -S. Sun, "The composition of Earth," Chem. Geol. **120**, 223–253 (1995).

A. Perepelov, M. Kuzmin, S. Tsypukova, Y. Shcherbakov, S. Dril, A. Didenko, E. Dalai-Erdene, M. Puzankov, and A. Zhgilev, "Late Cenozoic Uguumur and Bod–Uul volcanic centers in northern Mongolia: mineralogy, geochemistry, and magma sources," Minerals **10** (7), 612.

G. Perini, "Sr-isotope and micro-isotope analyses of minerals: examples from some mafic alkaline potassic rocks," Period. Mineral. **69**, 107–124 (2000).

C. Pin, B. Danielle, C. Bassin, and F. Poitrasson, "Contomitant separation of strontium and samarium-neodymium for isotopic analysis in silicate samples, based on specific extraction chromatography," Anal. Chem. Acta. **299**, 209–217 (1994).

S. V. Rasskazov, *Bazaltoids of Udokan* (Nauka Sib. Otd., Novosibirsk, 1985) [in Russian].

S. V. Rasskazov, *Magmatism of the Baikal Rift System* (Nauka, Novosibirsk, 1993) [in Russian].

S. V. Rasskazov and A. V. Ivanov, "Redox conditions of hot spot magmatism and extensional Zones of the Baikal rift system," *Precambrian Lithotectonic Complexes of East Siberia* (Irkutsk Univ., Irkutsk, 1998), pp. 44–58 [in Russian].

M. I. Renjith, "Micro-textures in plagioclase from 1994–1995 eruption, Barren Island Volcano: evidence of dynamic magma plumbing system in the Andaman subduction zone," Geosci. Front. **5**, 113–126 (2014).

H. Sheth, "Giant plagioclase basalts: continental flood basalt–induced remobilization of anorthositic mushes in a deep crustal sill complex," GSA Bull. **128** (5/6), 916–925.

F. M. Stupak, V. A. Lebedev, and E. A. Kudryashova, "Structural material complexes in the Late Cenozoic Udokan lava plateau: patterns of distribution and rock associations," J. Volcanol. Seismol. **6** (3), 172–183 (2012).

A. D. Sounders and M. J. Norry, "Chemical and isotopic systematics of oceanic basalts: implications for mantle composition and processes," in *Magmatism in the Ocean Basins,* Ed. by S. -S. Sun and W. F. McDonough, Geol. Soc. London, Sp. Publ. **42**, 313–345 (1989).

H. P. Taylor and S. M.F. Sheppard, "Igneous rocks: I. Processes of isotopic fractionation and isotope systematics," In: *Stable Isotopes in High Temperature Geological Processes,* Ed. by J. W. Valley, H. P. Taylor, and J. R. O'Neil, Rev. Mineral. **16**, 227–271 (1986).

F. J. Tepley, III, J. P. Davidson, and M. A. Clynne, "Magmatic interactions as recorded in plagioclase phenocrysts of Chaos Crags, Lassen volcanic center, California," J. Petrol. **40** (5), 787–806 (1999).

F. J. Tepley, III, J. P. Davidson, R. I. Tilling, and J. G. Arth, "Magma mixing, recharge, and eruption histories recorded in plagioclase phenocrysts from El Chichon Volcano, Mexico," J. Petrol. **41**, 1397–1411 (2000).

O. M. Turkina, A. D. Nozhkin, and T. B. Bayanova, "Sources and formation conditions of Early Proterozoic granitoids from the southwestern margin of the Siberian Craton," Petrology **14** (3), 262–283 (2006).

A. Vho, P. Lanari, and D. Rubatto, "An internally-consistent database for oxygen isotope fractionation between minerals," J. Petrol. **60** (11), 2101–2130 (2019).

N. Ya. Volyanyuk, B. M. Vladimirov, V. G. Semenova, and V. M. Novikov, "Anorthoclase megacrysts from basanites and problem of their genesis," Dokl. Akad. Nauk SSSR **240** (5), 938–941 (1978).

V. V. Yarmolyuk, V. G. Ivanov, V. I. Kovalenko, and B. G. Pokrovsky, "Magmatism and geodynamics of the southern Baikal volcanic region (mantle hot spot): results of geochronological, geochemical, and isotopic (Sr, Nd, and O) investigations," Petrology **11** (1), 1–30 (2003).

Z. F. Zhao and Y. F. Zheng, "Calculation of oxygen isotope fractionation in magmatic rocks," Chem. Geol. **193**, 59–80 (2003).

Translated by E. Kurdyukov